An Advanced Correlation Algorithm between GTEM and OATS for Radiated Emission Tests

Ae-kyoung Lee

CONTENTS

ABSTRACT

This paper proposes an algorithm to improve the correlation between giga-hertz transverse electromagnetic (GTEM) cell and open area test site (OATS). It is based on the dipole modeling process of an unknown source object in a GTEM cell and on the evaluation of the approximate far field equations correlated with measured GTEM powers at output port of the GTEM cell. In this algorithm, the relative phase differences between dipole moments play an important part in modeling the test object as a set of dipoles and offer stable calculation of emission values. The radiated emission test using this algorithm requires fifteen orientations of equipment under test, but the increased orientations as compared with the previous method have little effect on the time needed for testing. Radiation from a notebook computer has been tested for statistical analysis of the correlation between GTEM data and OATS data. The emission test results of the notebook computer show that the mean, the standard deviation, and the correlation coefficient are -0.62, 1.99, and $+0.85$, respectively. These figures indicate that this algorithm provides improved accuracy in the measurement of electromagnetic emissions over the previous method.

I. INTRODUCTION

An open area test site (OATS) is well suited for measurement of electromagnetic interference (EMI) but construction of a site with a low noise environment is getting more difficult and expensive as electronic and electric industry progresses. A semi-anechoic chamber (SAC) offers good performances at high frequencies because it has almost no reflections, and attenuates most of the ambient noise. But it does not have good low frequency performance and cannot eliminate resonance completely. Both an OATS and an SAC require much time to measure radiation from a test object because of direct measurements by antennas. A gigahertz transverse electromagnetic (GTEM) cell is serviceable and valuable as a substitute facility for either an OATS or an SAC. It has the following advantages: (1) it makes efficient use of space; (2) it will not cost a fortune to buy and maintain; (3) it offers good frequency performance and good ambient shielding; and (4) it is applicable to both radiated emission and radiated susceptibility measurements.

Radiated susceptibility testing using a GTEM cell is performed as in a TEM cell. But radiated emission testing with a GTEM cell needs its own specific GTEM algorithm, that is, a measurement method and formulation which yield equivalent results to other types of facilities, either an OATS or an SAC. A radiated emission test in a GTEM cell is to simulate OATS emission measurements by modeling the radiation from the equipment

under test (EUT) or a test object as that from an equivalent set of electric and magnetic dipoles. Recently, the Federal Communications Commission (FCC) announced that they will accept for compliance demonstration purposes, radiated emission measurements taken using a GTEM cell under the some conditions. Various studies of correlation are underway [1]-[6].

Correlation algorithms have been developed for TEM cells and GTEM cells by several researchers [1], [6]-[8]. Though all the phases and amplitudes of the dipole moment components are available using a TEM cell, TEM cells cannot be used for radiated emission testing for a general EUT owing to the limitation of the frequency bandwidth [9], [10]. A GTEM cell is a one port device as compared with a standard TEM cell. Therefore one cannot obtain the perfect information on dipole moments.

The previous algorithm [2] assumes that the six components of electric and magnetic dipole moments are basically in phase, but it has been experienced that all of the six moment components are not in phase at a number of frequency points when dipole moments are computed with GTEM measured powers. For most EUTs, it may be impossible for all moments to be in phase at all measuring frequencies.

This paper proposes a new algorithm for more efficient and accurate radiation emission testing. The proposed algorithm requires only the relative phase differences, not absolute phase values of dipole moment compo-

nents, through fifteen EUT orientations. It offers more stable emission evaluations than the previous algorithm [1], [6] and allows one to save time and test costs. This paper describes how the fifteen measured powers at the GTEM output port may be related to OATS emission measurement results, compares the GTEM results with the OATS data and shows a strong correlation between GTEM and OATS data.

II. CORRELATION ALGORITHM

Since the radiation from an electrically small source in a waveguide is well documented [8], [10], [11], only summarized theory will be described in Appendix A.
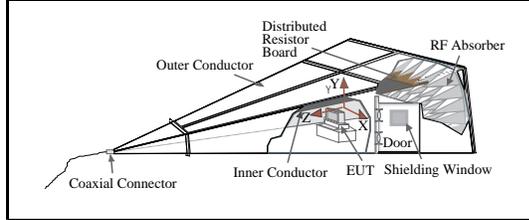

Fig. 1. GTEM cell.

The configuration of a standard GTEM cell is a tetrahedral shape with an inner conductor as shown in Fig. 1. The apex will be chosen as lying in the forward direction, +z.

The measured power at GTEM output port, normalized by $\frac{1}{4}e_{0y}(o)^2$ where $e_{0y}(o)$ is electric field y component of the fundamental mode at EUT location o when unit power is flowing across GTEM cell, is

$$|\widetilde{a_0}|^2 = |[P_y e^{j\psi_{py}} - jk_0 M_x e^{j\psi_{mx}}]|^2, \qquad (1)$$

where P_y and ψ_{py} are the amplitude and phase of y component of electric dipole moment $\mathbf{P}$, and M_x and ψ_{mx} have similar meanings for magnetic dipole moment $\mathbf{M}$. We know that the measured GTEM power, $|\widetilde{a_0}|^2$, is related to the current source, i.e., the electric and magnetic dipole moments. Differential EUT orientation in the GTEM cell will couple to differential dipole components and the TEM mode field $e_{0y}(o)$.

The measured GTEM power of (1) has the electrical information as to the EUT emissions in the GTEM cell. But full information, all the amplitudes and phases of electric and magnetic dipole moments, can not be obtained. So we have to devise theoretically the most suitable terms composed of amplitudes and phases of the dipole components required for the OATS emission simulation. The objective of OATS emission test is to measure the radiated vertical and horizontal electric field from an EUT in a far field zone over a ground screen and to compare the measured electric field with the specification limits. For a far field of free space, the approximate radiated electric fields from an EUT, as represented by a set of electric and magnetic dipoles, are as follows:

$$\mathbf{E} \simeq -j\omega\mathbf{A} \qquad (2)$$
$$\simeq -j\omega\mu_0 \frac{e^{-jk_0 r}}{4\pi r}[\mathbf{P} - jk_0\mathbf{a}_r \times \mathbf{M}],$$

where, $\mathbf{P} = P_x e^{j\psi_{px}}\mathbf{a}_x + P_y e^{j\psi_{py}}\mathbf{a}_y + P_z e^{j\psi_{pz}}\mathbf{a}_z$, $\mathbf{M} = M_x e^{j\psi_{mx}}\mathbf{a}_x + M_y e^{j\psi_{my}}\mathbf{a}_y + M_z e^{j\psi_{mz}}\mathbf{a}_z$, and $\mathbf{a}_r$, $\mathbf{a}_x$, $\mathbf{a}_y$ and $\mathbf{a}_z$ are unit vectors of each axis.
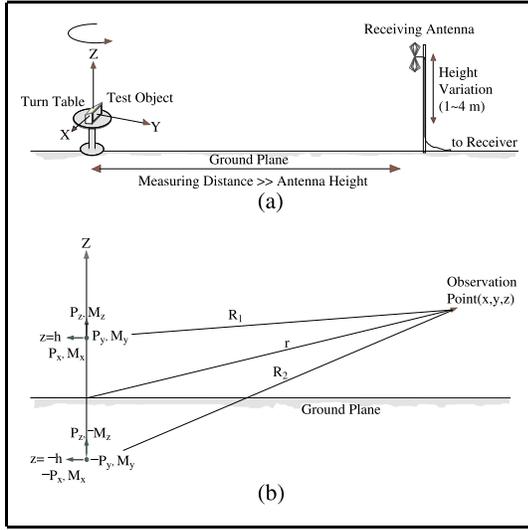
Fig. 2. (a) OATS radiated measurement configuration and (b) application of image theory to (a).

The region of our interest is over a ground screen as shown in Fig. 2, where both electric and magnetic sources and their image sources are to be included. The three components of the radiated electric field over a ground plane can be written as follows:

$$|E_x| \simeq \left| \left(\frac{\eta k_0}{4\pi}\right) \frac{e^{-jk_0 R_1}}{R_1} \left[-jP_x e^{j\psi_{px}} \right. \right.$$
$$\left. + k_0 \left(\frac{z_1}{R_1} M_y e^{j\psi_{my}} - \frac{y}{R_1} M_z e^{j\psi_{mz}} \right) \right]$$
$$+ \left(\frac{\eta k_0}{4\pi}\right) \frac{e^{-jk_0 R_2}}{R_2} \left[jP_x e^{j\psi_{px}} \right.$$
$$\left. \left. + k_0 \left(\frac{z_2}{R_2} M_y e^{j\psi_{my}} + \frac{y}{R_2} M_z e^{j\psi_{mz}} \right) \right] \right|,$$

(3-1)

$$|E_y| \simeq \left| \left(\frac{\eta k_0}{4\pi}\right) \frac{e^{-jk_0 R_1}}{R_1} \left[-jP_y e^{j\psi_{py}} \right. \right.$$
$$\left. + k_0 \left(\frac{x}{R_1} M_z e^{j\psi_{mz}} - \frac{z_1}{R_1} M_x e^{j\psi_{mx}} \right) \right]$$
$$+ \left(\frac{\eta k_0}{4\pi}\right) \frac{e^{-jk_0 R_2}}{R_2} \left[jP_y e^{j\psi_{py}} \right.$$

$$+ k_0 \left(-\frac{x}{R_2} M_z e^{j\psi_{mz}} - \frac{z_2}{R_2} M_x e^{j\psi_{mx}} \right) \right],$$

(3-2)

$$|E_z| \simeq \left| \left(\frac{\eta k_0}{4\pi}\right) \frac{e^{-jk_0 R_1}}{R_1} \left[-jP_z e^{j\psi_{pz}} \right. \right.$$
$$\left. + k_0 \left(\frac{y}{R_1} M_x e^{j\psi_{mx}} - \frac{x}{R_1} M_y e^{j\psi_{my}} \right) \right]$$
$$+ \left(\frac{\eta k_0}{4\pi}\right) \frac{e^{-jk_0 R_2}}{R_2} \left[-jP_z e^{j\psi_{pz}} \right.$$
$$\left. \left. + k_0 \left(\frac{y}{R_2} M_x e^{j\psi_{mx}} - \frac{x}{R_2} M_y e^{j\psi_{my}} \right) \right] \right|,$$

(3-3)

where subscripts 1 and 2 represent the real source and the image source respectively, η_0 and k_0 are the free space wave impedance and the propagation constant, respectively, and $z_1 = z - h$, $z_2 = z + h$.

The amplitude of vertical electric field, $|E_v|$, is $|E_z|$, and that of the horizontal electric field, $|E_h|$, is $\sqrt{|E_x|^2 + |E_y|^2}$. Unfortunately several terms in expansions of (3) are not available from the GTEM algorithm. But they are negligible for the case that measurement distance is much greater than the height of receiving antenna. The simulated equation over a ground screen for the correlation algorithm is as follows:

$$|E_v|^2 \simeq \left(\frac{\eta_0 k_0}{4\pi}\right)^2 \left\{ \frac{1}{R_1^2} \left[(P_z^2 + k_0^2 M_x^2) \left(\frac{y}{R_1}\right)^2 \right. \right.$$
$$+ (P_z^2 + k_0^2 M_y^2) \left(\frac{x}{R_1}\right)^2$$
$$- 2k_0^2 \frac{xy}{R_1^2} M_x M_y C_{mxy}$$
$$\left. + 2k_0 \left(\frac{y}{R_1} P_z M_x S_{zx} - \frac{x}{R_1} P_z M_y S_{zy} \right) \right]$$
$$+ \frac{1}{R_2^2} \left[(P_z^2 + k_0^2 M_x^2) \left(\frac{y}{R_2}\right)^2 \right.$$

$$+(P_z^2+k_0^2 M_y^2)\left(\frac{x}{R_2}\right)^2 - 2k_0^2 \frac{xy}{R_2^2} M_x M_y C_{mxy}$$

$$+2k_0\left(\frac{y}{R_2} P_z M_x S_{zx} - \frac{x}{R_2} P_z M_y S_{zy}\right)\Bigg]$$

$$+2\cos[k_0(R_1-R_2)]\left(\frac{1}{R_1 R_2}\right)^2$$

$$\times\Bigg[(P_z^2+k_0^2 M_x^2)y^2+(P_z^2+k_0^2 M_y^2)x^2$$

$$-2k_0^2 xy M_x M_y C_{mxy}+k_0(R_1+R_2)$$

$$\times(y P_z M_x S_{zx}-x P_z M_y S_{zy})\Bigg]\Bigg\}, \qquad (4)$$

$$|E_h|^2 \simeq \left(\frac{\eta_0 k_0}{4\pi}\right)^2 \Bigg\{\frac{1}{R_1^2}\Bigg[(P_x^2+k_0^2 M_y^2)\left(\frac{z_1}{R_1}\right)^2$$

$$+(P_y^2+k_0^2 M_x^2)\left(\frac{z_1}{R_1}\right)^2$$

$$+(P_x^2+k_0^2 M_z^2)\left(\frac{x}{R_1}\right)^2$$

$$+(P_y^2+k_0^2 M_z^2)\left(\frac{y}{R_1}\right)^2$$

$$-2k_0^2\left(\frac{yz_1}{R_1^2} M_y M_z C_{myz}+\frac{xz_1}{R_1^2} M_x M_z C_{mxz}\right)$$

$$+2k_0\left(\left(\frac{z_1}{R_1}\right)(P_x M_y S_{xy}-P_y M_x S_{yx})\right.$$

$$\left.-\frac{y}{R_1} P_x M_z S_{xz}+\frac{x}{R_1} P_y M_z S_{yz}\right)\Bigg]$$

$$+\frac{1}{R_2^2}\Bigg[(P_x^2+k_0^2 M_y^2)\left(\frac{z_2}{R_2}\right)^2$$

$$+(P_y^2+k_0^2 M_x^2)\left(\frac{z_2}{R_2}\right)^2$$

$$+(P_x^2+k_0^2 M_z^2)\left(\frac{x}{R_2}\right)^2$$

$$+(P_y^2+k_0^2 M_z^2)\left(\frac{y}{R_2}\right)^2$$

$$+2k_0^2\left(\frac{yz_1}{R_2^2} M_y M_z C_{myz}+\frac{xz_2}{R_2^2} M_x M_z C_{mxz}\right)$$

$$+2k_0\left(\left(\frac{z_2}{R_2}\right)(-P_x M_y S_{xy}+P_y M_x S_{yx})\right.$$

$$\left.-\frac{y}{R_2} P_x M_z S_{xz}+\frac{x}{R_2} P_y M_z S_{yz}\right)\Bigg]$$

$$+2\cos[k_0(R_1-R_2)]\left(\frac{1}{R_1 R_2}\right)^2$$

$$\times[k_0^2[M_y M_z C_{myz}(yz_1-yz_2)$$

$$+M_x M_z C_{mxz}(xz_1-xz_2)]$$

$$+k_0(R_1 z_2-R_2 z_1)(P_x M_y S_{xy}-P_y M_x S_{yx})$$

$$+(R_1+R_2)(y P_x M_z S_{xz}-x P_y M_z S_{yz})\Bigg]\Bigg\},$$

$$(5)$$

where, $C_{mab}=\cos(\psi_{ma}-\psi_{mb})$ and $S_{ab}=\sin(\psi_{pa}-\psi_{mb})$ which subscripts a and b may be either x, y or z.

The absolute phase values of dipole moments, ψ_{px}, ψ_{py}, ψ_{pz}, ψ_{mx}, ψ_{my}, and ψ_{mz} can not be obtained using GTEM cell but the terms including the relative phase differences of dipole moment components such as $P_x M_y S_{xy}$ and $M_x M_z C_{mxz}$ can be obtained by the presented algorithm. From (4) and (5), the number of the least and the most suitable terms is fifteen and thus fifteen independent orientations of the EUT in GTEM cell are required to obtain the equivalent OATS results. The correlation algorithm is to find the fifteen orientations of the EUT and link the fifteen measured GTEM powers and the OATS emission via (4) and (5). The following two sections will describe these two procedures respectively.

1. Determining the Test Object Orientations

A coordinate system (x, y, z) and a primed coordinate system (x', y', z') are referenced to

GTEM cell and EUT, respectively. The EUT positions in a GTEM cell must be devised to obtain the electric field of (4) and (5).

Five measurements, with the axis alignment, (xx', yy', zz'), are needed to determine the vertical radiated field of (4). The axis alignment, (xx', yy', zz'), means that the measurements start with conforming the EUT coordinate axes x', y' and z' to GTEM coordinate axes x, y and z respectively. Then the five counterclockwise rotations about y axis are performed with the five angles set at $0°$, $45°$, $90°$, $180°$, and $270°$, and the powers at the output port of GTEM cell for each rotated EUT are measured. Thus, the measured GTEM powers are related to the rotation angles as shown in Table 1 (a).

The procedure to get the horizontal electric field requires two axis alignments (xy', yz', zx') and (xz', yx', zy'). The first axis alignment, (xy', yz', zx'), means placing the y' axis of the EUT along the x axis of the GTEM cell, the z' axis along the y axis, and the x' axis along the z axis. Similarly, the second axis alignment, (xz', yx', zy'), means placing the z' axis of the EUT along the x axis of the GTEM cell, the x' axis along the y axis, and the y' axis along the z axis. Then, the same five rotations and the measurements for each axis alignment are performed with the total measurement number of ten. The five counterclockwise rotation angles about the y axis are $0°$, $45°$, $90°$, $180°$ and $270°$. The relation between EUT rotations and measured powers for the horizontal field is shown in Table 1 (b). The symbol Q_n represents the normalized power when an EUT has been rotated counterclockwise about the y axis through an angle ϕ_n.

The full fifteen equations are described in Appendix B. The fifteen GTEM measured powers $Q_n^{xx'}$, $Q_n^{xy'}$ and $Q_n^{xz'}$ ($n = 1, 2, \cdots, 5$) are correlated with the OATS emission of (4) and (5) in the following section.

2. Relating Measured Quantities to the Radiated Field

As shown in Figs. 1 and 2, the coordinate system of the OATS is defined differently from that of GTEM cell, and the relationship between GTEM quantities and OATS quantities are given in Appendix C.

The fifteen terms of the radiated electric field equations, (4) and (5), over the ground plane are expressed in the form of the measured GTEM powers.

The vertical electric field equation, (4), can be expressed with the five GTEM powers, P_{v1}, P_{v2}, $\cdots$, and P_{v5} composed of $Q_1^{xx'}$, $Q_2^{xx'}$, $\cdots$, and $Q_5^{xx'}$, as follows:

$$
\begin{aligned}
|E_v|^2 \simeq \left(\frac{\eta_o k_0}{4\pi}\right)^2 &\left\{\frac{1}{R_1^2}\left[P_{v2}\left(\frac{y}{R_1}\right)^2\right.\right. \\
&+ P_{v1}\left(\frac{x}{R_1}\right)^2 - 2\frac{xy}{R_1^2}P_{v5} \\
&\left. + 2\left(\frac{y}{R_1}P_{v4} - \frac{x}{R_1}P_{v3}\right)\right] \\
&+ \frac{1}{R_2^2}\left[P_{v2}\left(\frac{y}{R_2}\right)^2 + P_{v1}\left(\frac{x}{R_2}\right)^2\right. \\
&\left.\left. - 2\frac{xy}{R_2^2}P_{v5} + 2\left(\frac{y}{R_2}P_{v4} - \frac{x}{R_2}P_{v3}\right)\right]\right\}
\end{aligned}
$$

Table 1. EUT rotations for determining (a) the vertical electric field, and (b) the horizontal electric field.

(a)

axis alignment		$(xx',\ yy',\ zz')$
relation of the two coordinate systems (GTEM & EUT)		$\begin{bmatrix} x \\ y \\ z \end{bmatrix} = \begin{bmatrix} C\phi_n & 0 & S\phi_n \\ 0 & 1 & 0 \\ -S\phi_n & 0 & C\phi_n \end{bmatrix} \cdot \begin{bmatrix} x' \\ y' \\ z' \end{bmatrix}$
moment component	$P_y e^{j\psi_{py}}$	$P_y e^{j\psi_{py}} = P_{y'} e^{j\psi_{py'}}$
derivation from rotation	$M_x e^{j\psi_{mx}}$	$M_x e^{j\psi_{mx}} = M_{x'} e^{j\psi_{mx'}} C\phi_n + M_{z'} e^{j\psi_{mz'}} S\phi_n$
normalized power		$Q_n^{xx'} = P_{y'}^2 + k_0^2[M_{x'}^2 C^2\phi_n + M_{z'}^2 S^2\phi_n$ $+ 2M_{z'}M_{x'}C_{mz'x'}C\phi_n S\phi_n]$ $- 2k_0[P_{y'}M_{x'}S_{y'x'}C\phi_n$ $+ P_{y'}M_{z'}S_{y'z'}S\phi_n]$

$*$ $C\phi_n = \cos\phi_n$ and $S\phi_n = \sin\phi_n$

(b)

axis alignment		$(xy',\ yz',\ zx')$	$(xz',\ yx',\ zy')$
relation of the two coordinate systems (GTEM & EUT)		$\begin{bmatrix} x \\ y \\ z \end{bmatrix} = \begin{bmatrix} C\phi_n & 0 & S\phi_n \\ 0 & 1 & 0 \\ -S\phi_n & 0 & C\phi_n \end{bmatrix} \cdot \begin{bmatrix} y' \\ z' \\ x' \end{bmatrix}$	$\begin{bmatrix} x \\ y \\ z \end{bmatrix} = \begin{bmatrix} C\phi_n & 0 & S\phi_n \\ 0 & 1 & 0 \\ -S\phi_n & 0 & C\phi_n \end{bmatrix} \cdot \begin{bmatrix} z' \\ x' \\ y' \end{bmatrix}$
moment component	$P_y e^{j\psi_{py}}$	$P_y e^{j\psi_{py}} = P_{z'} e^{j\psi_{pz'}}$	$P_y e^{j\psi_{py}} = P_{x'} e^{j\psi_{px'}}$
derivation from rotation	$M_x e^{j\psi_{mx}}$	$M_x e^{j\psi_{mx}}$ $= M_{y'} e^{j\psi_{my'}} C\phi_n$ $+ M_{x'} e^{j\psi_{mx'}} S\phi_n$	$M_x e^{j\psi_{mx}}$ $= M_{z'} e^{j\psi_{mz'}} C\phi_n$ $+ M_{y'} e^{j\psi_{my'}} S\phi_n$
normalized power		$Q_n^{xy'} = P_{z'}^2$ $+ k_0^2[M_{y'}^2 C^2\phi_n + M_{x'}^2 S^2\phi_n$ $+ 2M_{x'}M_{y'}C_{mx'y'}C\phi_n S\phi_n]$ $- 2k_0[P_{z'}M_{y'}S_{z'y'}C\phi_n$ $+ P_{z'}M_{x'}S_{z'x'}S\phi_n]$	$Q_n^{xz'} = P_{x'}^2$ $+ k_0^2[M_{z'}^2 C^2\phi_n + M_{y'}^2 S^2\phi_n$ $+ 2M_{y'}M_{z'}C_{my'z'}C\phi_n S\phi_n]$ $- 2k_0[P_{x'}M_{z'}S_{x'z'}C\phi_n$ $+ P_{x'}M_{y'}S_{x'y'}S\phi_n]$

$$+2\cos[k_0(R_1-R_2)]\left(\frac{1}{R_1R_2}\right)^2$$

$$\times[P_{v2}\,y^2+P_{v1}x^2-2xyP_{v5}$$

$$+(R_1+R_2)(yP_{v4}-xP_{v3})]\Bigg\},\qquad(6\text{-}1)$$

where

$$P_{v1}=\frac{Q_1^{xx'}+Q_4^{xx'}}{2},$$

$$P_{v2}=\frac{Q_3^{xx'}+Q_5^{xx'}}{2},$$

$$P_{v3}=\frac{Q_4^{xx'}-Q_1^{xx'}}{4},$$

$$P_{v4}=\frac{Q_5^{xx'}-Q_3^{xx'}}{4},$$

$$\text{and}\quad P_{v5}=Q_2^{xx'}-\frac{Q_1^{xx'}+Q_3^{xx'}+Q_4^{xx'}+Q_5^{xx'}}{4}$$

$$-\frac{\sqrt{2}(Q_1^{xx'}+Q_3^{xx'}-Q_4^{xx'}-Q_5^{xx'})}{4}.$$

$$(6\text{-}2)$$

As expected, the horizontal electric field equation, (5), can be expressed in the form of the ten GTEM powers, P_{hm} $(m=1,\cdots,10)$, composed of $Q_n^{xy'}$ and $Q_n^{xz'}$ $(n=1,\cdots,5)$, as follows:

$$|E_h|^2\simeq\left(\frac{\eta_0k_0}{4\pi}\right)^2\Bigg\{\frac{1}{R_1^2}\Bigg[P_{h2}\left(\frac{z_1}{R_1}\right)^2+P_{h6}\left(\frac{z_1}{R_1}\right)^2$$

$$+P_{h1}\left(\frac{x}{R_1}\right)^2+P_{h7}\left(\frac{y}{R_1}\right)^2$$

$$-2\left(\frac{yz_1}{R_1^2}P_{h5}+\frac{xz_1}{R_1^2}P_{h10}\right)+2\left(\left(\frac{z_1}{R_1}\right)\right.$$

$$\times(P_{h4}-P_{h8})-\frac{y}{R_1}P_{h3}+\frac{x}{R_1}P_{h9}\Bigg)\Bigg]$$

$$+\frac{1}{R_2^2}\Bigg[P_{h2}\left(\frac{z_2}{R_2}\right)^2+P_{h6}\left(\frac{z_2}{R_2}\right)^2$$

$$+P_{h1}\left(\frac{x}{R_2}\right)^2+P_{h7}\left(\frac{y}{R_2}\right)^2$$

$$+2\left(\frac{yz_1}{R_2^2}P_{h5}+\frac{xz_2}{R_2^2}P_{h10}\right)+2\left(\left(\frac{z_2}{R_2}\right)\right.$$

$$\times\ (-P_{h4}+P_{h8})-\frac{y}{R_2}P_{h3}+\frac{x}{R_2}P_{h9}\Bigg)\Bigg]$$

$$+2\cos[k_0(R_1-R_2)]\left(\frac{1}{R_1R_2}\right)^2$$

$$\times[k_0^2[P_{h5}(yz_1-yz_2)+P_{h10}(xz_1-xz_2)]$$

$$+k_0(R_1z_2-R_2z_1)(P_{h4}-P_{h8})$$

$$+(R_1+R_2)(yP_{h3}-xP_{h9})]\Bigg\},\qquad(7\text{-}1)$$

where

$$P_{h1}=\frac{Q_1^{xy'}+Q_4^{xy'}}{2},$$

$$P_{h2}=\frac{Q_3^{xy'}+Q_5^{xy'}}{2},$$

$$P_{h3}=\frac{Q_4^{xy'}-Q_1^{xy'}}{4},$$

$$P_{h4}=\frac{Q_5^{xy'}-Q_3^{xy'}}{4},$$

$$P_{h5}=Q_2^{xy'}-\frac{Q_1^{xy'}+Q_3^{xy'}+Q_4^{xy'}+Q_5^{xy'}}{4}$$

$$-\frac{\sqrt{2}(Q_1^{xy'}+Q_3^{xy'}-Q_4^{xy'}-Q_5^{xy'})}{4},$$

$$P_{h6}=\frac{Q_1^{xz'}+Q_4^{xz'}}{2},$$

$$P_{h7}=\frac{Q_3^{xz'}+Q_5^{xz'}}{2},$$

$$P_{h8}=\frac{Q_4^{xz'}-Q_1^{xz'}}{4},$$

$$P_{h9}=\frac{Q_5^{xz'}-Q_3^{xz'}}{4},$$

$$\text{and}\quad P_{h10}=Q_2^{xz'}-\frac{Q_1^{xz'}+Q_3^{xz'}+Q_4^{xz'}+Q_5^{xz'}}{4}$$

$$-\frac{\sqrt{2}(Q_1^{xz'}+Q_3^{xz'}-Q_4^{xz'}-Q_5^{xz'})}{4}.$$

$$(7\text{-}2)$$

The above procedure completes the equivalent equations, (6) and (7), in accordance with the OATS emissions composed of the fifteen

GTEM powers. From (6) and (7), we can see that this algorithm does not need to find all the amplitudes of dipole moment components differently from the previous method [1].

It has been assumed in the previous GTEM algorithm [1] that the six components of electric and magnetic dipole moments are basically in phase and the moments squared are given as in (8-1) and (8-2). These are in the form of subtractions between the measured powers at the output port of a GTEM cell as follows:

$$M_{x'}^2 = \frac{(P_2 - P_4)(P_6 - P_8)}{k_0^2(P_{10} - P_{12})},$$

$$M_{y'}^2 = \frac{(P_6 - P_8)(P_{10} - P_{12})}{k_0^2(P_2 - P_4)},$$

$$M_{z'}^2 = \frac{(P_{10} - P_{12})(P_2 - P_4)}{k_0^2(P_6 - P_8)}, \qquad (8\text{-}1)$$

$$P_{x'}^2 = P_9 - k_0^2 M_{z'}^2 = P_{11} - k_0^2 M_{y'}^2,$$

$$P_{y'}^2 = P_1 - k_0^2 M_{x'}^2 = P_3 - k_0^2 M_{z'}^2,$$

$$P_{z'}^2 = P_5 - k_0^2 M_{y'}^2 = P_7 - k_0^2 M_{x'}^2, \qquad (8\text{-}2)$$

where $P_i(i=1, \cdots, 12)$ is the measured power at GTEM output port. All six moment components of (8-1) and (8-2) should have the same signs, whether they are plus or minus because it is assumed that they are in phase. But in the measurements of a notebook computer, we have experienced that the phases of the six moment components in (8) are out of accord with one another at a number of frequency points and the denominators of (8-1) were partially zero at some frequency points. We could not calculate the emission value from EUT at these frequency points. The reason for this lack of stability is that (8) is in the form of subtractions between powers when the dipole

moments, are evaluated. The correlation algorithm proposed here removes these problems and offers a stable calculation at all frequency points as shown in (6) and (7).

A notebook computer is tested by this algorithm and the results are compared with OATS data in the following chapter.

III. CORRELATION ANALYSIS AND DISCUSSION

We know from Fig. 3 that distributed resistor board and RF absorber within the GTEM cell minimize reflections and resonances but cannot remove them completely. The voltage standing wave ratio (VSWR) of the GTEM cell used here is less than 1.75 at the critical frequency and better than 1.5 at other frequencies for radiated emission testing as shown in Fig. 3 and it is similar to others commonly used.

The VSWR is not considered here for radiated emission results because it is too slight to have an effect on the measured power.

1. Comparison of GTEM and OATS Data

A notebook computer is selected as a sample EUT. The radiated emission results for a notebook computer are compared with OATS data.

A notebook computer is tested under the condition of reading data—"H" strings—from its floppy disk and hard disk and writing them on the display unit unceasingly by software.
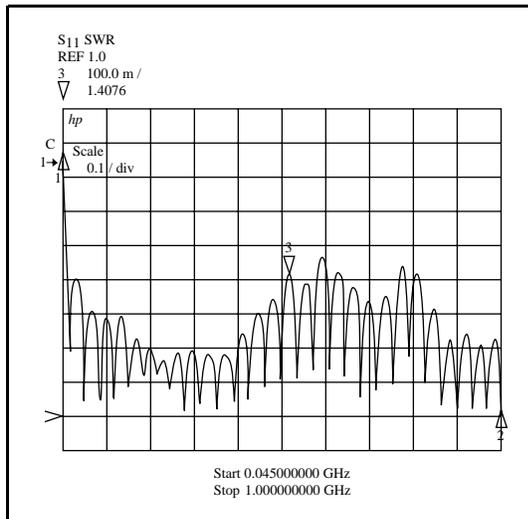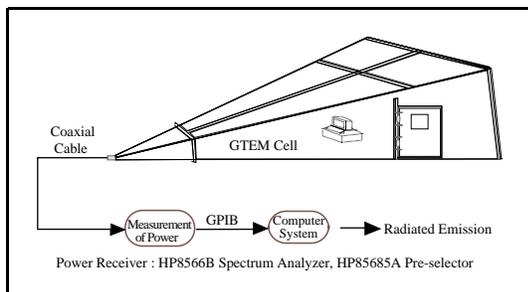
Fig. 3. VSWR of the GTEM cell used.

Fig. 4. Radiated emission measuring system using the GTEM cell.

Fig. 5. Radiated emission results from a notebook computer (486SX GNC425C, Gold Star) as determined from GTEM cell measurements; (a) vertical electric field strength (dB V/m) and (b) horizontal electric field strength (dB V/m).

Figures 5 (a) and (b) are vertical and horizontal radiated emission distributions from a notebook computer with power line. The number of total data points are 2002, 1001 points 30~300 MHz and 1001 points at 300~1000 MHz. The power receiver holds the maximum values at each EUT position. These data from GTEM cell are transmitted to computer system via general purpose interface bus (GPIB) cable and computed by a program written in Quick BASIC and Fortran languages . The required time for the measurement of all these performances is less than one hour. The source height was 0.8 m and measuring distance was 3 m for both the simulation by GTEM cell and measurement at an OATS. Two receiving antennas, a biconical antenna for the band of 30~300 MHz and a log-periodic array antenna for the band of 300~1000 MHz, were used at the OATS. The antenna height was varied from 1 m to 4 m with 20 cm steps and the turn table is remotely controlled and continuously rotated at about 1.7 rpm. In the calculation, the rotation step is set at intervals of 10

mum values for each antenna setting. This procedure is repeated four times, that is, vertical and horizontal arrangements of both biconical and log-periodic array antennas. Figure 5 is the GTEM emission simulated results for the entire frequencies. Table 2 makes a comparison between GTEM data and OATS data for all the bounding values within about 10 dB of the maximum emission peak value.

One of the advantages of radiated emission testing using a GTEM cell is to offer three dimensional field views at any frequency point and this is useful for considering electromagnetic interference (EMI) countermeasures for the EUT. An enormous amount of time may be required to get three dimensional field distribution information at an OATS. As an example, Figure 6 shows the simulated vertical (649.30 MHz) and horizontal (250.32 MHz) electric field distributions, when the measuring distance is 3 m.

2. Statistical Analysis of GTEM to OATS Correlation

For a statistical correlation analysis between GTEM and OATS, the mean μ and the standard deviation σ as the statistics of the differences and the linear correlation coefficient r (also called Pearson's r) are calculated for each tables of the above section [12], [13]. This statistical analysis is one of the several steps that must be accomplished to obtain the FCC permission to use GTEM data for formal compliance testing. The linear correlation coefficient is most widely used and is given by the for-
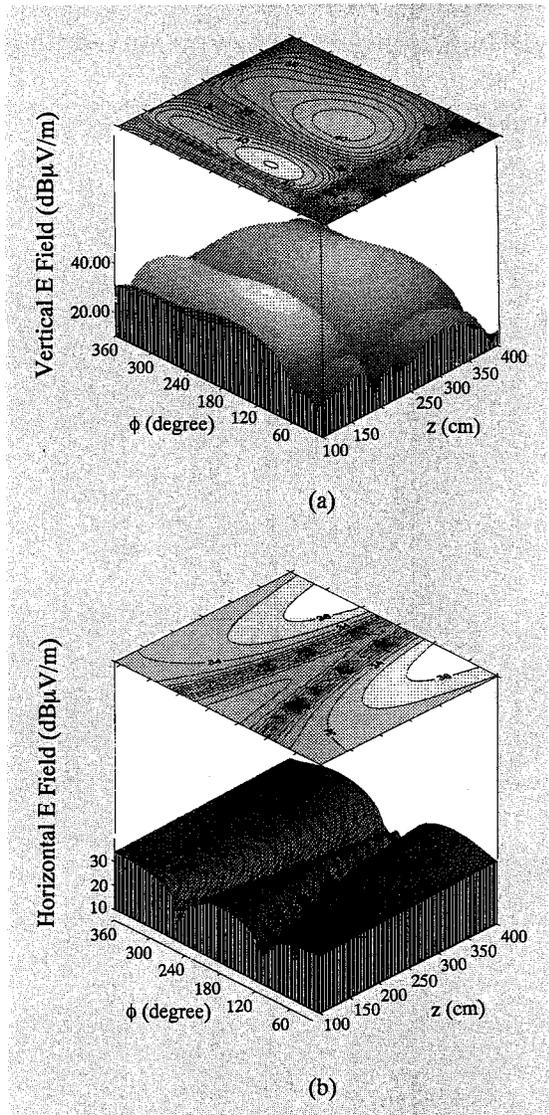

Fig. 6. 3-dimensional views of electric field radiation from the notebook computer; (a) the radiated vertical component ($f = 649.30$ MHz), and (b) the radiated horizontal component ($f = 250.32$ MHz).

mula

$$r = \frac{\Sigma_i (x_i - \bar{x})(y_i - \bar{y})}{\sqrt{\Sigma_i (x_i - \bar{x})^2}\sqrt{\Sigma_i (y_i - \bar{y})^2}}, \qquad (9)$$

Table 2(a). Comparison of vertical electric fields radiated from a notebook computer (486SX GNC425C, Gold Star).

Frequency (MHz)	GTEM data (dBμV/m)	OATS data (dBμV/m)	Difference(dB) (GTEM-OATS)	Frequency (MHz)	GTEM data (dBμV/m)	OATS data (dBμV/m)	Difference(dB) (GTEM-OATS)
34.86	39.84	44.98	-5.14	301.40	36.93	36.62	+0.31
38.64	38.43	41.06	-2.63	308.40	36.24	35.36	+0.88
41.88	34.76	36.90	-2.14	325.20	36.62	35.23	-1.39
45.66	36.97	39.13	-2.16	350.40	40.69	37.65	+3.04
48.90	35.35	38.63	-3.28	364.40	39.24	36.73	+2.51
52.68	29.77	33.64	-3.87	392.40	38.35	35.34	+3.01
55.92	37.25	40.37	-3.12	399.40	40.08	37.23	+2.85
59.43	30.70	34.47	-3.77	499.80	39.27	38.50	+0.77
62.94	36.07	37.24	-1.17	500.20	40.18	38.60	+1.58
66.72	34.85	34.86	-0.01	549.90	38.96	38.05	+0.91
69.96	32.96	31.01	+1.95	555.50	37.18	37.53	-0.35
73.74	33.49	31.63	+1.86	600.30	40.51	39.59	+0.92
77.52	33.69	32.66	+1.03	637.40	39.18	39.24	-0.06
84.00	32.36	35.25	-2.89	649.30	44.02	39.99	+4.03
100.20	33.83	34.29	-0.46	750.80	41.20	41.44	-0.24
112.62	32.05	35.53	-3.48	773.90	40.77	41.64	-0.87
140.70	33.08	35.55	-2.47	799.80	41.37	41.14	+0.23
150.42	32.61	35.72	-3.12	864.20	41.14	42.71	+1.57
168.78	36.52	36.87	-0.35	892.90	41.44	42.31	-0.87
196.86	32.80	37.65	-4.85	907.06	41.04	42.93	-1.89
224.40	38.11	40.05	-1.94	918.80	42.89	42.82	+0.07
242.22	36.26	38.06	-1.80	925.80	42.31	42.59	-0.28
245.46	36.51	37.68	-1.17	937.70	42.00	43.19	-1.19
249.78	43.38	42.13	+1.25	953.80	42.66	43.76	-1.10
273.54	39.76	39.11	+0.65	961.50	42.12	43.57	-1.45
275.70	39.41	38.94	+0.47	979.00	42.24	43.81	-1.57
300.00	38.30	40.15	-1.85	982.50	42.35	43.41	-1.06

* In Table 2, the OATS data were collected by biconial antenna (BBA 9106 in VHA 9103 holder, made by Schwartzbeck Mess-Electronik) at 30~300 MHz, and by log-periodic array antenna (Model 3146, made by EMCO) at 300 MHz~1 GHz.

Table 2(b). Comparison of horizontal electric fields radiated from a notebook computer (486SX GNC425C, Gold Star).

Frequency (MHz)	GTEM data (dBμV/m)	OATS data (dBμV/m)	Difference(dB) (GTEM-OATS)	Frequency (MHz)	GTEM data (dBμV/m)	OATS data (dBμV/m)	Difference(dB) (GTEM-OATS)
34.86	36.75	38.63	-1.88	392.40	36.97	36.69	+0.28
38.64	36.01	35.36	+0.65	399.40	37.32	37.74	-0.42
41.88	33.25	33.50	-0.25	448.40	38.06	38.87	-0.81
45.66	34.89	33.39	+1.50	500.20	39.57	39.80	-0.23
48.90	33.43	32.49	+0.94	547.80	38.91	39.61	-0.70
62.94	34.81	30.30	+4.51	601.00	39.08	39.24	-0.16
84.54	34.12	31.24	+2.88	650.70	39.64	40.08	-0.44
91.02	31.89	29.75	+2.14	700.40	42.99	41.55	+1.44
94.80	31.06	29.79	+1.27	728.40	39.25	41.39	-2.14
105.60	29.78	31.65	-1.87	770.40	40.11	41.99	-1.88
245.46	34.25	38.33	-4.08	800.50	40.28	41.55	-1.27
250.32	39.94	43.78	-3.84	841.10	40.72	42.32	-1.60
325.20	34.00	35.83	-1.83	845.30	40.02	42.45	-2.43
350.40	35.09	36.55	-1.46	848.80	40.32	42.73	-2.41
353.20	34.04	35.30	-1.26	854.40	40.15	42.59	-2.44
363.70	35.40	36.28	-0.88				

mula

$$r = \frac{\Sigma_i(x_i - \bar{x})(y_i - \bar{y})}{\sqrt{\Sigma_i(x_i - \bar{x})^2}\sqrt{\Sigma_i(y_i - \bar{y})^2}}, \qquad (9)$$

where, x_i is GTEM data in $dB\mu V/m$ and y_i is OATS data at each frequency point, and x is the mean of x_i's and y is the mean of y_i's. The value of r lies between -1 and $+1$, inclusive. It takes on a value of 1, termed "complete positive correlation." The means and the standard devia-tions for the differences between GTEM data and OATS data, and Pearson's r's for all cases are presented at the Table 3.

The power line contribution of EUT in the GTEM cell differs much from that at the OATS. That is not considered in this study. Nonetheless, the mean and standard devia-tion average of all differences (GTEM-OATS) written at table 2 are -0.62 dB and 1.99 dB re-

Table 3. GTEM to OATS Correlation.

		mean(μ) (dB)	standard deviation (σ) (dB)	Pearson's r
Vertical	30~300 MHz	-1.65	1.98	+0.81
Component	300~1000 MHz	+0.37	1.63	+0.89
Horizontal	30~300 MHz	+1.64	2.64	+0.82
Component	300~1000 MHz	1.09	1.03	+0.90

spectively. And the correlation coefficient is +0.85. If Pearson's r is +0.7 or higher, this indicates that there is a very strong correlative relationship between the two sets of data [5].

Tables 4 (a) and (b) are results extracted from [3] and [5], respectively.

Table 4. (a) Correlation coefficients for phones (ROLM Company) [3], (b) comparison of GTEM to OATS (EMCO) [5].

(a)

	model 1	model 2
GTEM 1 - OATS	+0.70	+0.62
GTEM 2 - OATS	+0.74	+0.67

(b)

mean	+1.70
standard deviation	3.19
correlation coefficient	+0.43

Although it is unreasonable to compare the

statistical results directly with others because EUTs, the numbers of data and the frequency bands are mutually different from each other. Table 3 shows a trend that the present results are better when compared with others.

IV. CONCLUSION

This paper proposes a new algorithm for improved correlation of radiated emission between OATS and GTEM cell and shows that this algorithm offers enough accuracy to overcome not only the limits of space, time, cost and ambient noise of OATS but also the shortcomings of the previous GTEM method.

It is normally considered impossible to find the full dipole information of an EUT because a GTEM cell is a single port device. Thus this algorithm approximately evaluates the far field equations composed of phases as well as amplitudes of dipole moments which are electrical quantities of the EUT. It has been supposed that the measurement distance is much

greater than the height of receiving antenna. The optimum EUT orientations in GTEM cell then have been tracked to determine unknown terms composed of amplitudes and phases of the dipole moments in equations. The total number of orientations is fifteen and the same number of powers at output port of the GTEM cell for the EUT orientations could be correlated with the unknown terms of the approximate far field equations, that is, the OATS emission equations.

For an experimental study, the measurements of radiated emission from a notebook computer over the OATS were performed at 3 m distance and the measured OATS data were compared with GTEM calculated ones for the same measuring distance. As a result, for all data within about 10 dB of the maximum emission peak value, a set of data for the OATS and the GTEM cell showed significantly high correlation coefficient of $+0.85$. The correlation coefficient, or Pearson's r, is one of the statistical evaluation parameters of the FCC. For a complex or large system and a special test object such as a microwave oven, this algorithm is to be further refined because it is not trivial to tilt in a steep slope. This aspect needs further study.

APPENDIX A: MULTI-POLE MODELING OF MEASURED POWER AT GTEM PORT

Electrically small radiator may be characterized by three equivalent orthogonal electric dipole moments and three equivalent orthogonal magnetic dipole moments. When an unknown source object is placed at the center in a waveguide (GTEM cell) whose cross section is similar to an asymmetric TEM cell as shown in Fig. 1, its radiated energy couples into the fundamental transmission mode and propagates toward the output port of the GTEM cell. The electric and magnetic fields excited in the waveguide may be expressed as:

$$\mathbf{E}^{(\pm)} = \sum_n \begin{bmatrix} a_n \\ b_n \end{bmatrix} \mathbf{E}_n^{(\pm)}, \qquad \text{(A1-1)}$$

$$\mathbf{H}^{(\pm)} = \sum_n \begin{bmatrix} a_n \\ b_n \end{bmatrix} \mathbf{H}_n^{(\pm)}, \qquad \text{(A1-2)}$$

where, $\mathbf{E}_n^{(\pm)}$ and $\mathbf{H}_n^{(\pm)}$ are respectively the vector orthogonal electric and magnetic basis functions describing the field structure for the nth mode in the waveguide, and a_n and b_n are the expansion coefficients. But the only fields in forward direction $(+z)$, $E_n^{(+)}$ and $H_n^{(+)}$ are available, since a GTEM cell is a one port device, so the field radiated in the positive z direction is

$$\mathbf{E}^{(+)} = \sum_n a_n \mathbf{E}_n^{(+)}, \qquad \text{(A2-1)}$$

$$\mathbf{H}^{(+)} = \sum_n a_n \mathbf{H}_n^{(+)}. \qquad \text{(A2-2)}$$

Let the field structure functions for the nth mode propagated in the positive z direction be represented as follows:

$$\mathbf{E}_n^{(+)} = (\mathbf{e}_n + \mathbf{e}_{zn})e^{-jk_n z}, \qquad \text{(A3-1)}$$

$$\mathbf{H}_n^{(+)} = (\mathbf{h}_n + \mathbf{h}_{zn})e^{-jk_n z} \qquad \text{(A3-2)}$$

where k_n is the propagation constant of the nth mode, and $\mathbf{e}_n$ and $\mathbf{h}_n$ are the transverse vector functions of the rectangular coordinates. It will be assumed that the transverse vector functions are normalized and orthogonal, so that

$$\int_s [\mathbf{e}_m \times \mathbf{h}_n] \cdot \widehat{\mathbf{z}} dS = \delta_{mn}, \qquad (A4)$$

where the integration is over the guide cross section S and δ_{mn} is the Kronecker delta function.

The expansion coefficient a_n is obtained, with an application of the Lorentz reciprocity principle [11],

$$a_n = -\frac{1}{2} \int_v \mathbf{J}(r') \cdot \mathbf{E}_n^{(-)}(r') dv', \qquad (A5)$$

where $\mathbf{J}(r')$ is the current density. If the modes of interest are nearly uniform over the source volume and the current source is placed at $z = 0$, a_n can be obtained as follows:

$$a_n = -\frac{1}{2} \left\{ \mathbf{E}_n^-(o) \cdot \int_v \mathbf{J}(r') dv' \right.$$
$$\left. + \int_v [\mathbf{r}' \cdot \nabla \mathbf{E}_n^-(o)] \cdot \mathbf{J}(r') dv' \right\}. \quad (A6)$$

Since the current source is electrically small,

$$a_n = -\frac{1}{2} \left\{ \mathbf{E}_n^{(-)}(o) \cdot \mathbf{P} - jk_n \eta_0 \mathbf{H}_n^{(-)}(o) \cdot \mathbf{M} \right.$$
$$\left. + \frac{1}{2} \nabla \mathbf{E}_n^{(-)}(o) : \vec{\mathbf{Q}} \right\}, \qquad (A7)$$

where $\mathbf{P}$ is the electric dipole moment, $\mathbf{M}$ is the magnetic dipole moment, $\vec{\mathbf{Q}}$ is the dyadic electric quadrupole moment and the double dot, ":" means the double inner product between the two dyadic components, $\nabla \mathbf{E}_n^{(-)}(o)$, and $\vec{\mathbf{Q}}$. $\vec{\mathbf{Q}}$ can be neglected for a perfectly uniform field over the electrically small source [12].

In general, the six components of the dipole moments, i.e., P_x, P_y, P_z, M_x, M_y, and M_z, would be independent of phase, so let them be represented as follows:

$$\mathbf{P} = P_x e^{j\psi_{px}} \mathbf{a}_x + P_y e^{j\psi_{py}} \mathbf{a}_y$$
$$+ P_z e^{j\psi_{pz}} \mathbf{a}_z, \qquad (A8\text{-}1)$$
$$\mathbf{M} = M_x e^{j\psi_{mx}} \mathbf{a}_x + M_y e^{j\psi_{my}} \mathbf{a}_y$$
$$+ M_z e^{j\psi_{mz}} \mathbf{a}_z. \qquad (A8\text{-}2)$$

If the TEM mode is primarily dominant in a GTEM cell, the wave impedance is η_0 and the x component of the transverse vector function for the TEM mode, $e_{0x}(o)$ is zero at the center of a GTEM cell, so that,

$$a_0 = -\frac{1}{2}(P_y e^{j\psi_{py}} - jk_0 M_x e^{j\psi_{mx}}) e_{0y}(o). \quad (A9)$$

where subscript, 0 of a_0 and e_{0y} signifies TEM mode. Because the $e_{0y}(o)$ is a vertical electric field strength at origin, o for 1 watt input power, from (A3),

$$e_{0y}(o) = \frac{\sqrt{Z_0}}{h} \qquad (A10)$$

where h is a height from the floor to the septum at the location of current source in the GTEM cell and Z_0 is the characteristic impedance of the GTEM cell, 50Ω [6].

The measured power at GTEM output port normalized by $\frac{1}{4} e_{0y}(o)^2$ is

$$|\tilde{a}_0|^2 = |[P_y e^{j\psi_{py}} - jk_0 M_x e^{j\psi_{mx}}]|^2. \qquad (1)$$

APPENDIX B: POWERS VIA EUT ROTATIONS

From three axis alignments and five rota-

Table I. Relation of GTEM to OATS quantities (a) for vertical field and (b) for horizontal field.

(a)

OATS quantities	GTEM quantities	measured GTEM powers
$P_z^2 + k_0^2 M_y^2$	$P_{y'}^2 + k_0^2 M_{x'}^2$	$P_{v1} = \dfrac{Q_1^{xx'} + Q_4^{xx'}}{2}$
$P_z^2 + k_0^2 M_x^2$	$P_{y'}^2 + k_0^2 M_{z'}^2$	$P_{v2} = \dfrac{Q_3^{xx'} + Q_5^{xx'}}{2}$
$k_0 P_z M_y \sin(\psi_{pz} - \psi_{my})$	$k_0 P_{y'} M_{x'} \sin(\psi_{py'} - \psi_{mx'})$	$P_{v3} = \dfrac{Q_4^{xx'} - Q_1^{xx'}}{4}$
$k_0 P_z M_x \sin(\psi_{pz} - \psi_{mx})$	$k_0 P_{y'} M_{z'} \sin(\psi_{py'} - \psi_{mz'})$	$P_{v4} = \dfrac{Q_5^{xx'} - Q_3^{xx'}}{4}$
$k_0^2 M_x M_y \cos(\psi_{mx} - \psi_{my})$	$k_0^2 M_{x'} M_{z'} \cos(\psi_{mx'} - \psi_{mz'})$	$P_{v5} = Q_2^{xx'} - \dfrac{Q_1^{xx'} + Q_3^{xx'} + Q_4^{xx'} + Q_5^{xx'}}{4}$ $- \dfrac{\sqrt{2}(Q_1^{xx'} + Q_3^{xx'} - Q_4^{xx'} - Q_5^{xx'})}{4}$

(b)

OATS quantities	GTEM quantities	measured GTEM powers
$P_x^2 + k_0^2 M_z^2$	$P_{z'}^2 + k_0^2 M_{y'}^2$	$P_{h1} = \dfrac{Q_1^{xy'} + Q_4^{xy'}}{2}$
$P_x^2 + k_0^2 M_y^2$	$P_{z'}^2 + k_0^2 M_{x'}^2$	$P_{h2} = \dfrac{Q_3^{xy'} + Q_5^{xy'}}{2}$
$k_0 P_x M_z \sin(\psi_{px} - \psi_{mz})$	$k_0 P_{z'} M_{y'} \sin(\psi_{pz'} - \psi_{my'})$	$P_{h3} = \dfrac{Q_4^{xy'} - Q_1^{xy'}}{4}$
$k_0 P_x M_y \sin(\psi_{px} - \psi_{my})$	$k_0 P_{z'} M_{x'} \sin(\psi_{pz'} - \psi_{mx'})$	$P_{h4} = \dfrac{Q_5^{xy'} - Q_3^{xy'}}{4}$
$k_0^2 M_y M_z \cos(\psi_{my} - \psi_{mz})$	$k_0^2 M_{y'} M_{x'} \cos(\psi_{my'} - \psi_{mx'})$	$P_{h5} = Q_2^{xy'} - \dfrac{Q_1^{xy'} + Q_3^{xy'} + Q_4^{xy'} + Q_5^{xy'}}{4}$ $- \dfrac{\sqrt{2}(Q_1^{xy'} + Q_3^{xy'} - Q_4^{xy'} - Q_5^{xy'})}{4}$
$P_y^2 + k_0^2 M_x^2$	$P_{x'}^2 + k_0^2 M_{z'}^2$	$P_{h6} = \dfrac{Q_1^{xz'} + Q_4^{xz'}}{2}$
$P_y^2 + k_0^2 M_z^2$	$P_{x'}^2 + k_0^2 M_{y'}^2$	$P_{h7} = \dfrac{Q_3^{xz'} + Q_5^{xz'}}{2}$
$k_0 P_y M_x \sin(\psi_{py} - \psi_{mx})$	$k_0 P_{x'} M_{z'} \sin(\psi_{px'} - \psi_{mz'})$	$P_{h8} = \dfrac{Q_4^{xz'} - Q_1^{xz'}}{4}$
$k_0 P_y M_z \sin(\psi_{py} - \psi_{mz})$	$k_0 P_{x'} M_{y'} \sin(\psi_{px'} - \psi_{my'})$	$P_{h9} = \dfrac{Q_5^{xz'} - Q_3^{xz'}}{4}$
$k_0^2 M_x M_z \cos(\psi_{mx} - \psi_{mz})$	$k_0^2 M_{y'} M_{z'} \cos(\psi_{my'} - \psi_{mz'})$	$P_{h10} = Q_2^{xz'} - \dfrac{Q_1^{xz'} + Q_3^{xz'} + Q_4^{xz'} + Q_5^{xz'}}{4}$ $- \dfrac{\sqrt{2}(Q_1^{xz'} + Q_3^{xz'} - Q_4^{xz'} - Q_5^{xz'})}{4}$

tion angles for each axis alignment in Table 1, we obtain the following fifteen normalized powers at GTEM port. From Table 1 (a) and (b), (B1) and (B2) are obtained respectively. The subscripts 1, 2, $\cdots$, and 5 mean the positions of EUT for five rotations and superscripts xx', xy' and xz' are axis alignments as stated above.

$$Q_1^{xx'} = P_{y'}^2 + k_0^2 M_{x'}^2 - 2k_0 P_{y'} M_{x'} \sin(\psi_{py'} - \psi_{mx'}),$$

$$Q_2^{xx'} = P_{y'}^2 + k_0^2 \left(\frac{1}{2} M_{x'}^2 + \frac{1}{2} M_{z'}^2 \right.$$
$$+ M_{x'} M_{z'} \cos(\psi_{mx'} - \psi_{mz'}) \bigg)$$
$$- \sqrt{2} k_0 (P_{y'} M_{x'} \sin(\psi_{py'} - \psi_{mx'})$$
$$+ P_{y'} M_{z'} \sin(\psi_{py'} - \psi_{mz'})),$$

$$Q_3^{xx'} = P_{y'}^2 + k_0^2 M_{z'}^2 - 2k_0 P_{y'} M_{z'} \sin(\psi_{py'} - \psi_{mz'}),$$

$$Q_4^{xx'} = P_{y'}^2 + k_0^2 M_{x'}^2 + 2k_0 P_{y'} M_{x'} \sin(\psi_{py'} - \psi_{mx'}),$$

$$\text{and } Q_5^{xx'} = P_{y'}^2 + k_0^2 M_{z'}^2 + 2k_0 P_{y'} M_{z'} \sin(\psi_{py'} - \psi_{mz'}).$$
$$(B1)$$

$$Q_1^{xy'} = P_{z'}^2 + k_0^2 M_{y'}^2 - 2k_0 P_{z'} M_{y'} \sin(\psi_{pz'} - \psi_{my'}),$$

$$Q_2^{xy'} = P_{z'}^2 + k_0^2 \left(\frac{1}{2} M_{y'}^2 + \frac{1}{2} M_{x'}^2 \right.$$
$$+ M_{y'} M_{x'} \cos(\psi_{my'} - \psi_{mx'}) \bigg)$$
$$- \sqrt{2} k_0 (P_{z'} M_{y'} \sin(\psi_{pz'} - \psi_{my'})$$
$$+ P_{z'} M_{y'} \sin(\psi_{pz'} - \psi_{my'})),$$

$$Q_3^{xy'} = P_{z'}^2 + k_0^2 M_{x'}^2 - 2k_0 P_{z'} M_{x'} \sin(\psi_{pz'} - \psi_{mx'}),$$

$$Q_4^{xy'} = P_{z'}^2 + k_0^2 M_{y'}^2 + 2k_0 P_{z'} M_{y'} \sin(\psi_{pz'} - \psi_{my'}),$$

$$Q_5^{xy'} = P_{z'}^2 + k_0^2 M_{x'}^2 + 2k_0 P_{z'} M_{x'} \sin(\psi_{pz'} - \psi_{mx'}),$$

$$Q_1^{xz'} = P_{x'}^2 + k_0^2 M_{z'}^2 - 2k_0 P_{x'} M_{z'} \sin(\psi_{px'} - \psi_{mz'}),$$

$$Q_2^{xz'} = P_{x'}^2 + k_0^2 \left(\frac{1}{2} M_{z'}^2 + \frac{1}{2} M_{y'}^2 \right.$$
$$+ M_{z'} M_{y'} \cos(\psi_{mz'} - \psi_{my}) \bigg)$$
$$- \sqrt{2} k_0 (P_{x'} M_{z'} \sin(\psi_{px'} - \psi_{mz'})$$
$$+ P_{x'} M_{y'} \sin(\psi_{px'} - \psi_{my'})),$$

$$Q_3^{xz'} = P_{x'}^2 + k_0^2 M_{y'}^2 - 2k_0 P_{x'} M_{y'} \sin(\psi_{px'} - \psi_{my'}),$$

$$Q_4^{xz'} = P_{x'}^2 + k_0^2 M_{z'}^2 + 2k_0 P_{x'} M_{z'} \sin(\psi_{px'} - \psi_{mz'}),$$

$$\text{and } Q_5^{xz'} = P_{x'}^2 + k_0^2 M_{y'}^2 + 2k_0 P_{x'} M_{y'} \sin(\psi_{px'} - \psi_{my'}).$$
$$(B2)$$

APPENDIX C: RELATION OF GTEM TO OATS QUANTITIES

From comparison of Figs. 1 and 2, we know that the axes x, y and z of OATS coordinate system correspond to the axes z, x and y of GTEM coordinate system respectively. As shown in Table I, the OATS dipole moment quantities in (4) and (5) for emission have relation with GTEM quantities which are also composed of measured GTEM powers.

REFERENCES

[1] P. Wilson, D. Hansen and D. Koenigstein, "Simulating open area test site emission measurements based on data obtained in a novel broadband TEM cell", *in Proc. IEEE 1989 Nat. Symp. on Electromagn. Compat.,* Denver, CO, May 1989, pp. 171-177.

[2] Edwin L. Brunaugh and John D. M. Osburn, "Radiated emissions test performance of the GHz TEM cell", *in Proc. IEEE 1991 Int. Symp. on Electromagn. Compat.,* Cherry Hill, NJ, Aug. 1991, pp. 1-7

[3] H. Stephen Berger, "Radiated emissions test correlation between G-TEM, SAC and OATS facilities using digital phones," *in Proc. IEEE 1993 Int. Symp. on Electromagn. Compat.,* Dallas, TX, Aug. 1993, pp. 295-297

[4] H. Stephen Berger, "A variable position, gravity down G-TEM configuration," *in Proc. 11th Int. Zurich Symp. and Technical Exhibition on Electromagn. Compat.,* Mar. 1995, pp. 465-470

[5] Edwin L. Bronaugh, John D. M. Osburn, "Statistical correlation requirements for determining acceptable performance of wide bandwidth TEM cells," *in Proc. EMC/ESD 1994 Int. Symp., Anaheim. Calif.,* Apr. 12-15, 1994, pp 99-104.

[6] P. Wilson, "On Correlating TEM Cell and OATS Emission Measurements," *IEEE Trans. Electromagn. Compat.,* vol. EMC-37, no. 1, pp 1-16, Feb. 1995.

[7] Mark T. Ma and Galen H. Koepke, "A method to quantify the radiation characteristics of an unknown interference source", National Bureau Standards (now NIST), Boulder, CO, Tech. Note TN-1059, Oct. 1982.

[8] Ippalapalli Sreenivasiah, David C. Chang, Mark T. Ma, "Emission characteristics of electrically small radiating sources from tests inside a TEM cell," *IEEE Trans. on Electromagn. Compat.,* vol. 23, no.3, pp 113-121, Aug. 1981

[9] Motohisa Kanda and R. David Orr, "Generation of standard Electromagnetic Fields in a TEM cell", National Bureau Standards (now NIST), Boulder, CO, Tech. Note TN-1319, Aug. 1988.

[10] Ae-kyoung Lee and Ki-kon Yang, "The characteristic impedance and the electric field uniformity of a GTEM cell", *the Journal of the Korean Institute of Communication Sciences*, vol. 19, no.3, pp. 523-532, Mar. 1994.

[11] R. E. Collin, *Field Theory of Guided Waves*. New York: McGraw Hill, 1960.

[12] William H., Brian P. Flannery, Saul A. Teukolsky and William T. Vetterling, *Numerical Recipes*, Cambridge University Press, 1986

[13] Ae-kyoung Lee, Sang-Hai Yi and Jung-ki Kim, "The bandwidth limitations of the TEM cell due to higher order modes", *Journal of the Korea Institute of Telematics and Electronics*, vol. 28-A, no.11, pp. 12-19, Nov. 1991.

Ae-kyoung Lee received B. S. and M. S. degrees in electronics engineering from Chung-Ang University, Seoul, Korea, in 1990 and in 1992, respectively. Since 1992, She has been in the department of Electromagnetic Compatibility engineering of ETRI. Her research interests include electromagnetic theory and numerical analysis of Electromagnetic Interference phenomena.